

21-Telluraporphyrins. 1. Impact of 21,23-Heteroatom Interactions on Electrochemical Redox Potentials, ^{125}Te NMR Spectra, and Absorption Spectra

Masako Abe, David G. Hilmey, Corey E. Stilts, Dinesh K. Sukumaran,* and Michael R. Detty*

Department of Chemistry, University at Buffalo, The State University of New York, Buffalo, New York 14260-3000

Received March 22, 2002

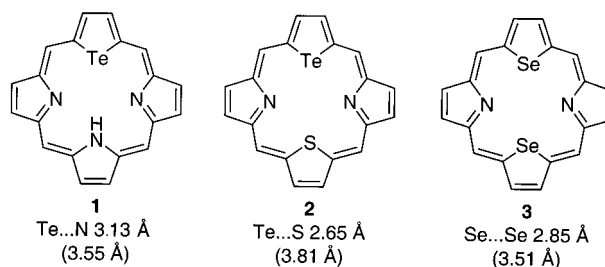
meso-Tetraphenyl-21-chalcogenaporphyrins **4–6** (S, Se, and Te as 21-chalcogen atoms, respectively) and *meso*-tetraphenyl-21,23-dichalcogenaporphyrins **7–10** [(S,S), (Se,S), (Se,Se), and (Te,S) combinations as 21,23-chalcogen atoms, respectively] were prepared by condensation of the appropriate 2,5-bis(phenylhydroxymethyl)chalcogenophene **11** with (1) benzaldehyde, pyrrole, tetrachlorobenzoquinone (TCBQ), and boron trifluoride etherate for the preparation of **4–6** or (2) the appropriate 2,5-bis(1-phenyl-1-pyrrolomethyl)chalcogenophene **13**, TCBQ, and boron trifluoride etherate for the preparation of **7–10**. Electrochemical oxidation and reduction potentials were measured by cyclic voltammetry for **4–10** and indicated that oxidation of 21-telluraporphyrins **6** and **10** was more facile (more cathodic) than for the other analogues in the series and **10** was more readily oxidized than **6**. The band I absorption maxima of 21-telluraporphyrins **6** and **10** were at shorter wavelengths than those of the corresponding analogues containing only sulfur and/or selenium chalcogen atoms. The extinction coefficients, ϵ , of the Soret bands of **6** and **10** were 7.6×10^4 and $7.2 \times 10^4 \text{ M}^{-1} \text{ cm}^{-1}$, respectively, which is significantly smaller than analogues **4**, **5**, and **7–9**, which have corresponding values of $>2 \times 10^5 \text{ M}^{-1} \text{ cm}^{-1}$. The ^{125}Te NMR spectrum of **6** gave a chemical shift of δ 834. Oxidation of **6** to oxotelluraporphyrin **12** gave a ^{125}Te NMR chemical shift of δ 1045. 21-Tellura-23-thiaporphyrin **10** gave a ^{125}Te NMR chemical shift of δ 1039, perhaps reflecting deshielding of the Te nucleus by the less than van der Waals contact with the S nucleus.

Introduction

Organotellurides are catalysts for the activation of H_2O_2 .¹ Oxidation of tellurium with H_2O_2 is followed by ligand exchange and reductive elimination of the new ligand as an oxidized species with regeneration of the organotelluride, which can then reenter the catalytic cycle.^{1c,d} The rate-determining step for the catalytic cycle in some systems appears to be the rate of oxidation of the organotelluride with H_2O_2 and, in others, the rate of reductive elimination. However, substituents that accelerate oxidation of the organotelluride also retard reductive elimination of the oxidized species, creating a conundrum with respect to catalyst design.²

The tellurium-containing 21- and 21,23-core-modified porphyrins represent an interesting class of molecules that should function as catalysts for the activation of H_2O_2 . In these molecules, a tellurium atom in the 21-

Chart 1



position has replaced one of the pyrrole N-H groups and is opposite an NH or S atom at the 23-position.³ The heteroatom at the 23-position can facilitate oxidation of the tellurium atom at the 21-position through donation of a lone-pair of electrons. The core-modified porphyrins of Chart 1 have intramolecular 21,23-heteroatom contacts that are less than the sum of van der Waals radii as the heteroatoms become larger (3.13 Å

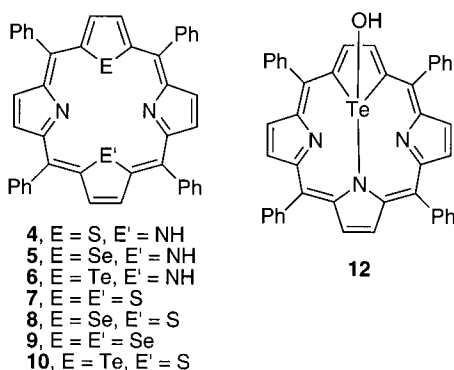
* To whom correspondence should be addressed. Fax: (716) 645-6963. E-mail: mdetty@acsu.buffalo.edu; dks@acsu.buffalo.edu.

(1) (a) Detty, M. R.; Gibson, S. L. *J. Am. Chem. Soc.* **1990**, *112*, 4086. (b) Detty, M. R.; Gibson, S. L. *Organometallics* **1992**, *11*, 2147. (c) Detty, M. R.; Friedman, A. E.; Oseroff, A. *J. Org. Chem.* **1994**, *59*, 8245. (d) Detty, M. R.; Zhou, F.; Friedman, A. E. *J. Am. Chem. Soc.* **1996**, *118*, 313. (e) Higgs, D. E.; Nelen, M. I.; Detty, M. R. *Org. Lett.* **2001**, *3*, 349. (f) Francavilla, C.; Drake, M. D.; Bright, F. V.; Detty, M. R. *J. Am. Chem. Soc.* **2001**, *123*, 57.

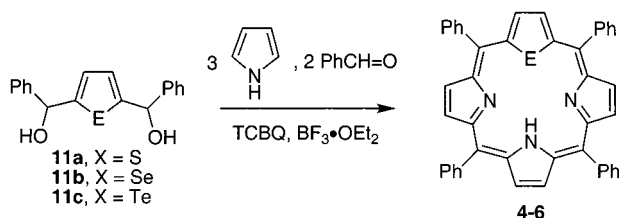
(2) Leonard, K. A.; Zhou, F.; Detty, M. R. *Organometallics* **1996**, *15*, 4285.

(3) (a) Ulman, A.; Manassen, J.; Frolow, F.; Rabinovich, D. *Tetrahedron Lett.* **1978**, 167. (b) Ulman, A.; Manassen, J.; Frolow, F.; Rabinovich, D. *Tetrahedron Lett.* **1978**, 1885. (c) Ulman, A.; Manassen, J. *J. Chem. Soc., Perkin Trans. 1* **1979**, *4*, 1066. (d) Latos-Grazynski, L.; Pacholska, E.; Chmielewski, P. J.; Olmstead, M. M.; Balch, A. L. *Inorg. Chem.* **1996**, *35*, 566. (e) Jeyaprakash Narayanan, S.; Sridevi, B.; Chandrashekar, T. K.; Vij, A.; Roy, R. *J. Am. Chem. Soc.* **1999**, *121*, 9053. (f) Pandian, R.; Chandrashekar, T. K. *J. Chem. Soc., Dalton Trans.* **1993**, 119.

Chart 2



Scheme 1



for Te...N distances in **1**,⁴ 2.65 Å for Te...S distances in **2**,^{3b} and 2.85 Å for Se...Se distances in **3**^{3a}). The larger van der Waals radii of the heteroatoms in the core-modified porphyrins enforce 21-heteroatom–23-heteroatom contact (sum of van der Waals radii in parentheses in Chart 1).^{3a,b,4}

Structures **1** and **2** of Chart 1 are constructed such that oxidation of tellurium by H₂O₂ should be facilitated by the 23-heteroatom, which can donate an electron pair to the oxidized chalcogen center. In fact, the air-oxidation of *meso*-tetraaryl-21-telluraporphyrins has been described as well as the crystal structure of a stable 21-oxo-21-telluraporphyrin.⁴ In this article, we compare selected chemical and spectral properties of several 21-chalcogena- and 21,23-dichalcogenaporphyrins, which underscore the 21,23-interactions of heteroatoms.

Results and Discussion

Preparation of 21-Chalcogenaporphyrins. Tetraphenyl-21-chalcogenaporphyrins **4–6** and 21,23-dichalcogenaporphyrins **7–10** were examined in this study (Chart 2). As shown in Scheme 1, 21-thiaporphyrin **4** and 21-selenaporphyrin **5** were each prepared in 12% isolated yield from benzaldehyde, pyrrole, and a 2,5-bis(phenylhydroxymethyl)chalcogenophene **11**^{4,5} using literature procedures.^{6,7}

The core-modified porphyrins produce singlet oxygen efficiently upon irradiation.⁵ In view of the facile oxida-

tion of related telluraporphyrin structures,⁴ the synthesis of previously unreported tetraphenyl-21-telluraporphyrin **6** was conducted in the dark to prevent the generation of singlet oxygen following formation of **6**. 2,5-Bis(phenylhydroxymethyl)tellurophene **11c**^{3b} was condensed with 3 equiv of pyrrole and 2 equiv of benzaldehyde in the presence of tetrachlorobenzoquinone (TCBQ) and BF₃·etherate to give **6** in 6% isolated yield following purification by chromatography and recrystallization. If the reaction mixture is exposed to light, oxidized telluraporphyrin **12** (Chart 2) is formed during the course of reaction.

Characterization of 6 and Its Product of Air-Oxidation 12. The ¹H NMR spectrum of **6** displayed the two tellurophene protons as a singlet at δ 10.4, the two pyrrole ring protons bearing the 23-NH as a doublet at δ 8.63 (*J* = 2 Hz for HN–C–C–CH in the pyrrole), and the four remaining pyrrole protons as an AB pattern at δ 8.60 and 8.56 with *J*_{AB} = 6.5 Hz. The aromatic protons appeared as two overlapping two-proton signals for the *ortho*-protons centered at δ 8.22 and two overlapping three-proton signals for the *meta*- and *para*-protons centered at δ 7.78. The NH proton appeared as a broadened singlet at δ –1.60, and the shielding is indicative that the 21-telluraporphyrin still maintains a diamagnetic ring current. The high-resolution electrospray mass spectrum of **6** gave *m/z* 730.1498, which is consistent with a molecular formula of C₄₄H₂₉N₃–130Te + H⁺ (calcd *m/z* of 730.1500). The ¹³C NMR spectrum of **6** displayed 16 discrete signals (18 expected), consistent with the symmetry expected for **6**.

The ¹²⁵Te NMR spectrum of **6** gave a signal at δ 834 (relative to δ 0.0 for Me₂Te). Other tellurophene and benzotellurophene ¹²⁵Te NMR chemical shifts have been reported to be in the δ 727–960 range, which suggests that the ¹²⁵Te NMR chemical shift of **6** is “typical” for tellurophenes.⁸

Upon standing in air-saturated CDCl₃, the ¹H NMR signals associated with **6** were replaced by a new spectrum consisting of a two-proton singlet at δ 10.5 corresponding to the two tellurophene ring protons, an AB pattern for four of the pyrrole ring protons at δ 8.47 and 8.44 with *J*_{AB} = 4.4 Hz, and a broadened singlet for two pyrrole ring protons at δ 8.31. These changes are consistent with air-oxidation of **6** to give an oxidized 21-telluraporphyrin **12**. The X-ray crystal structure of a structure related to **12** has been reported and shows the proton transfer from the pyrrole NH to the oxygen of the telluroxide.⁴ In the ¹H NMR spectrum of **12**, the long-range coupling of the pyrrole N–H with the 3,4–C–H's is no longer observed, which is consistent with proton transfer from nitrogen to oxygen and formation of the N–Te–O bond in structure **12**. The high-resolution electrospray mass spectrum of **12** gave *m/z* 746.1446, which is consistent with a molecular formula of C₄₄H₂₉–N₃O¹³⁰Te + H⁺ (calcd *m/z* of 746.1451) and oxidation of the tellurium atom.

The ¹²⁵Te NMR spectrum of **12** gave a signal at δ 1045, which is 211 ppm downfield from the ¹²⁵Te NMR signal of **6**. The chemical shift of **12** is similar to 2,5-

(4) Latos-Grazynski, L.; Pacholska, E.; Chmielewski, P. J.; Olmstead, M. M.; Balch, A. L. *Angew. Chem., Int. Ed. Engl.* **1995**, *34*, 2252.

(5) (a) Stilts, C. E.; Nelen, M. I.; Hilmey, D. G.; Davies, S. R.; Gollnick, S. O.; Oseroff, A. R.; Gibson, S. L.; Hilf, R.; Detty, M. R. *J. Med. Chem.* **2000**, *43*, 2403. (b) Hilmey, D. G.; Abe, M.; Nelen, M. I.; Stilts, C. E.; Baker, G. A.; Baker, S. N.; Bright, F. V.; Davies, S. R.; Gollnick, S. O.; Oseroff, A. R.; Gibson, S. L.; Hilf, R.; Detty, M. R. *J. Med. Chem.* **2002**, *45*, 449.

(6) Latos-Grazynski, L.; Lisowski, J.; Olmstead, M. M.; Balch, A. L. *Inorg. Chem.* **1989**, *28*, 1183.

(7) Latos-Grazynski, L.; Pacholska, E.; Chmielewski, P. J.; Olmstead, M. M.; Balch, A. L. *Inorg. Chem.* **1996**, *35*, 566.

(8) (a) Martin, M. L.; Trierweiler, M.; Galasso, V.; Fringuelli, F.; Taticchi, A. *J. Magn. Reson.* **1982**, *47*, 504. (b) Baiwir, M.; Llabres, G.; Luxen, A.; Christiaens, L.; Piette, J.-L. *Org. Magn. Reson.* **1984**, *22*, 312.

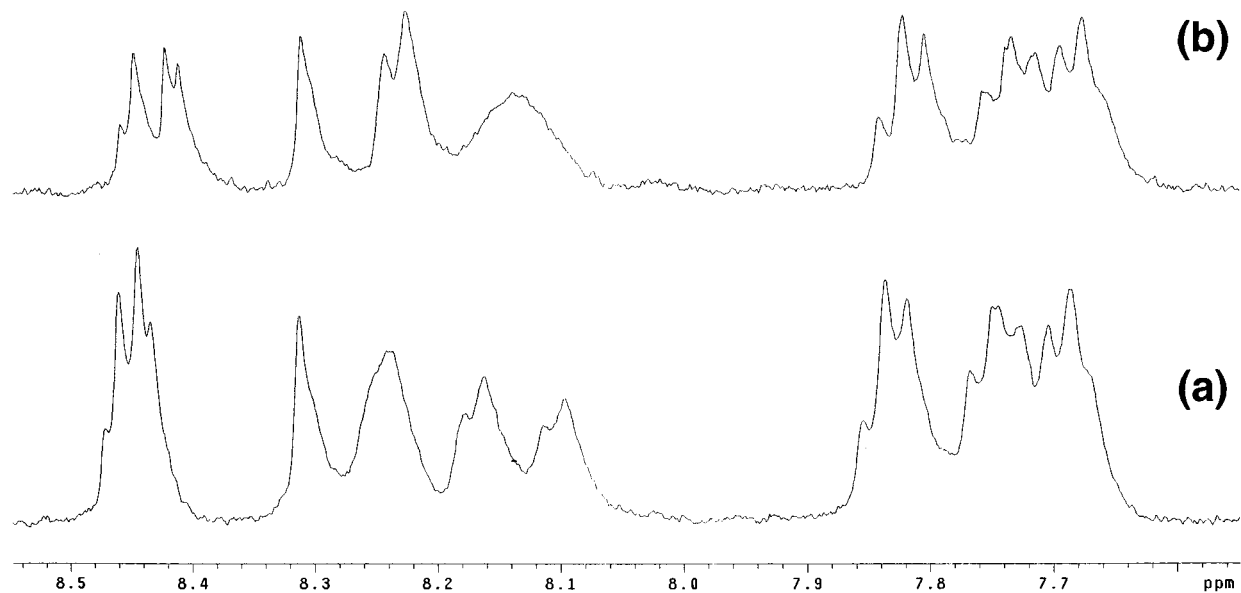
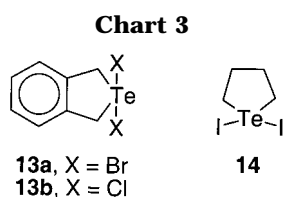


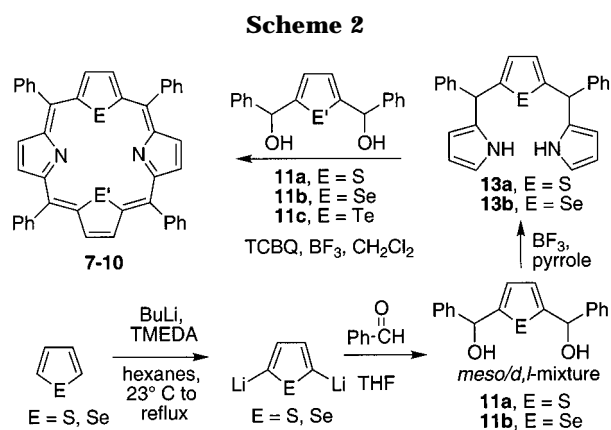
Figure 1. Variable-temperature ^1H NMR spectra for the δ 8.55–7.55 region for oxidized 21-telluraporphyrin **12** at (a) 21.5 $^\circ\text{C}$ and at (b) 60.0 $^\circ\text{C}$. The broadened doublets at δ 8.17 and 8.11 for the *ortho*-protons on the phenyl substituents adjacent to the tellurophene ring in (a) have collapsed to a single signal at δ 8.15 in (b) due to rotation of the phenyl substituents.



dihydrobenzotellurophene dihalides **13** (δ 940 for **13a** and δ 994 for **13b** relative to δ 0.0 for Me_2Te)⁹ and tetrahydrotellurophene diiodide **14** (δ 929),¹⁰ which have Te(IV) in a five-membered ring with two electronegative ligands (Chart 3).

The ^1H NMR signals from the protons of the phenyl substituents at the *meso* positions of **12** are also consistent with structure **12**. At 21.5 $^\circ\text{C}$, there are three distinct signals at δ 8.25, 8.17, and 8.11 in a 4:2:2 ratio for the *ortho*-phenyl protons (“doublet” structure) and several overlapping patterns in the range δ 7.9–7.6 for the *meta*- and *para*-protons (Figure 1a). Hindered rotation of the phenyl substituents around the *meso*-carbons leads to chemical nonequivalence for the *ortho*-protons of the phenyl groups adjacent to the oxidized tellurophene ring. One *ortho*-proton on each phenyl is proximal to the Te–O bond orthogonal to the tellurophene ring, while the other *ortho*-proton on each phenyl is proximal to the long Te \cdots N interaction. The phenyl substituents at the *meso*-positions between the pyrrole rings are far enough removed from the Te–O bond that all four *ortho*-protons appear to be chemically equivalent.

As shown in Figure 1b, heating the CDCl_3 solution of **12** to 60 $^\circ\text{C}$ leads to a sharper doublet at δ 8.24 for the *ortho*-protons of the phenyl substituents at the *meso*-positions between the pyrrole rings. The ^1H NMR signals at δ 8.17 and 8.11 for the *ortho*-protons of the



phenyl groups adjacent to the oxidized tellurophene ring at 21.5 $^\circ\text{C}$ collapse to a single signal at δ 8.15 at 60 $^\circ\text{C}$, from rotation of the phenyl substituents.

Preparation and Characterization of 21,23-Chalcogenaporphyrins 7–10. 5,10,15,20-Tetraphenyl 21,23-dichalcogenaporphyrins **7–10** were prepared by literature procedures as shown in Scheme 2.^{3a,b,8} The condensation of diols **11a**⁵ and **11b**⁵ with pyrrole in the presence of BF_3 -etherate gave bis(pyrrolomethyl)chalcogenophenes **15a** and **15b** in 46% and 51% isolated yields, respectively. The condensation of the appropriate diol **11** with bis(pyrrolomethyl)thiophene **15a** in the presence of TCBQ and BF_3 -etherate gave the known 21-,23-dithiaporphyrin **7**^{3b,e} in 17% isolated yield, the previously unknown 21-selena-23-thiaporphyrin **8** in 6% isolated yield, and the known 21-tellura-23-thiaporphyrin **10**^{3b} in 8% isolated yield. The condensation of **11b** with bis(pyrrolomethyl)selenophene **15b** gave the known 21,23-diselenaporphyrin **9**^{3b} in 12% isolated yield.

The ^1H NMR spectrum of 21-selena-23-thiaporphyrin **8** displayed a singlet at δ 9.94 for the selenophene protons, a singlet at δ 9.60 for the two thiophene protons, and an AB pattern of two protons each at δ 8.75 and 8.70 ($J_{\text{AB}} = 4$ Hz) for the four pyrrole protons,

(9) Zumbulyadis, N.; Gysling, H. J. *J. Organomet. Chem.* **1980**, *192*, 183.

(10) Al-Rubaie, A. Z.; Alshirayda, H. A.; Granger, P.; Chapelle, S. *J. Organomet. Chem.* **1985**, *287*, 321.

Table 1. Absorption Maxima, λ_{max} nm ($\epsilon \times 10^{-3}$, $\text{M}^{-1} \text{cm}^{-1}$), for 21-Chalcogenaporphyrins 4–6, 21,23-Dichalcogenaporphyrins 7–10, Oxidized 21-Telluraporphyrin 12, and Tetraphenylporphyrin 16 in Dichloromethane

compd	Soret	band IV	band III	band II	band I
4	425 (445)	515 (22.4)	550 (7.2)	616 (4.0)	675 (7.2)
5	425 (441)	515 (23.1)	551 (6.8)	618 (4.1)	677 (7.3)
6	438 (76.0)	482 (sh)	534 (11.2)	628 (5.5)	657 (6.4)
7	434 (190)	513 (19.3)	546 (5.5)	632 (4.0)	695 (7.5)
8	434 (210)	513 (21.0)	545 (5.8)	631 (4.1)	695 (7.2)
9	434 (221)	513 (22.4)	546 (6.2)	631 (4.2)	703 (7.5)
10	445 (71.6)	505 (sh)	545 (sh)	626 (4.2)	686 (3.7)
12	464 (87.1)	484 (63.5)	563 (6.6)	627 (sh)	655 (18.1)
16	411 (464)	511 (23.4)	545 (10.0)	588 (6.8)	646 (5.8)

which is consistent with the expected spectrum for the molecule. The four phenyl substituents appeared as two sets of overlapping signals centered at δ 8.23 for the *meta*-protons and δ 7.80 for the *ortho*- and *para*-protons. The high-resolution electrospray mass spectrum of **8** gave m/z 697.1215, which is consistent with a molecular formula of $\text{C}_{44}\text{H}_{28}\text{N}_2\text{S}^{80}\text{Se} + \text{H}^+$ (calcd m/z of 697.1217).

The short intramolecular contact of the 21,23-heteroatoms in **10** (2.65 Å for $\text{Te}\cdots\text{S}$)^{3b} might be expected to alter electron density at the heteroatoms. In particular, the more electronegative sulfur atom might pull electron density away from tellurium, effectively deshielding the tellurium atom. The ¹²⁵Te NMR spectrum of 21-tellura-23-thiaporphyrin **10** gave a signal at δ 1039 (relative to Me_2Te), which is significantly downfield of the ¹²⁵Te NMR signal from **6** (δ 833) and other tellurophenes.⁸ The ¹³C NMR chemical shifts of the carbon atoms of 21-telluraporphyrin **6** and 21-tellura-23-thiaporphyrin **10** were very similar, suggesting that electron densities are comparable in the carbon π -frameworks of **6** and **10**.

Electronic Absorption Spectra. The absorption maxima for the Soret band and the longer-wavelength bands I–IV are compiled in Table 1 for 21-chalcogenaporphyrins **4–6**, 21,23-dichalcogenaporphyrins **7–10**, and, for the purpose of comparison, tetraphenylporphyrin (**16**). All bands for 21-thiaporphyrin **4** and 21-selenaporphyrin **5** (Chart 1) are at longer wavelengths than tetraphenyl porphyrin **16**, with the greatest differences observed in the maxima of bands I and II, which are ~ 30 nm longer (Table 1). For 21-telluraporphyrin **6**, the band I absorption maximum is only about 10 nm longer than band I of tetraphenyl porphyrin **16**, while band II of **6** is about 40 nm longer than band II for **15**. For 21,23-core-modified porphyrins **7–10**, band I maxima are at 40–70 nm longer wavelengths still than tetraphenyl porphyrin **16**.

For porphyrin **15**, 21-chalcogenaporphyrins **4** and **5**, and 21,23-dichalcogenaporphyrins **7–9**, the Soret bands have very intense absorption ($\epsilon \approx 400\,000 \text{ M}^{-1} \text{cm}^{-1}$ for **4**, **5**, and **16** and $\epsilon \approx 200\,000 \text{ M}^{-1} \text{cm}^{-1}$ for **7–9**). The introduction of a tellurium atom into the core gives a pronounced decrease in the Soret band extinction coefficient (ϵ of $76\,000 \text{ M}^{-1} \text{cm}^{-1}$ for **6** and ϵ of $71\,600 \text{ M}^{-1} \text{cm}^{-1}$ for **10**) and a slight increase in λ_{max} for the Soret band (Table 1). The band I absorption maxima for **6** and **10** are slightly blue shifted, and the extinction coefficients are reduced relative to **4** and **5** for **6** or **7–9** for **10** (Table 1). One might expect the increased size of the tellurium atom to lead to a distortion in the

Table 2. Electrochemical Oxidation and Reduction Potentials for 21-Chalcogenaporphyrins 4–6, 21,23-Dichalcogenaporphyrins 7–10, and Tetraphenylporphyrin 16^a

compd	oxidation		reduction			
	E_{ox}		E_1°		E_2°	
	E_p^a , V	E_p^c , V	E_p^c , V	E_p^a , V	E_p^c , V	E_p^a , V
4	+1.05	+0.98 ^b	-1.18	-1.12	-1.45	-1.39
5	+1.09		-1.13	-1.07	-1.45	-1.39
6	+0.81		-1.06	-0.94 ^{b,c}	-1.67	-1.55 ^{b,c}
7	+1.13	+1.06 ^b	-1.10	-1.04	-1.40	-1.34
8	+1.12	+1.06 ^b	-1.07	-1.01	-1.36	-1.30
9	+1.10		-1.04	-0.98	-1.31	-1.25
10	+0.69		-1.03	-0.97	-1.29	-1.23
16	+1.02	+0.94 ^b	-1.36	-1.30	-1.69	-1.63

^a Dichloromethane solutions of $5 \times 10^{-4} \text{ M}$ analyte and 0.2 M Bu_4NBF_4 at a 1 mm Pt-disk electrode with a scan speed of 0.1 V s^{-1} . Peak potentials are reported vs Fc/Fc^+ ($E^\circ = +0.40 \text{ V}$). ^b Quasi-reversible with $i_p^c/i_p^a < 0.8$ for oxidations or $i_p^a/i_p^c < 0.8$ for reductions. ^c Scan speed of 0.5 V s^{-1} ; irreversible at 0.1 V s^{-1} .

planarity of the 21-telluraporphyrin and the 21-tellura-23-thiaporphyrin cores, which is perhaps reflected in the decreased intensity of the Soret band and band I absorptions. Selected spectra are compiled in the Supporting Information.

Oxidation of **6** to give oxotelluraporphyrin **12** gave a 26 nm red shift in the Soret band (λ_{max} of 438 nm for **6** vs 464 nm for **12**) with comparable extinction coefficients. The band I absorption maximum was little changed upon oxidation. However, the extinction coefficient of band I for **12** was nearly triple that of **6** (ϵ of $6400 \text{ M}^{-1} \text{cm}^{-1}$ for **6** vs ϵ of $18\,100 \text{ M}^{-1} \text{cm}^{-1}$ for **12**) and suggests that the heteroatom is part of the band I chromophore.

Electrochemical Oxidation and Reduction Potentials. The facile air-oxidation of **6** and related structures⁴ suggests that the electronegative nitrogen atom of the pyrrole at position 23 of the porphyrin is perhaps involved in the oxidation. We measured electrochemical oxidation and reduction potentials by cyclic voltammetry for 21-chalcogenaporphyrins **4–6**, 21,23-dichalcogenaporphyrins **7–10**, and tetraphenyl porphyrin **16**. Dichloromethane solutions ($5 \times 10^{-4} \text{ M}$) of compounds **4–10** and **15** with 0.2 M tetrabutylammonium fluoroborate as supporting electrolyte were run at a Pt-disk electrode using the ferrocene/ferrocinium couple (Fc/Fc^+ , $E^\circ = +0.40 \text{ V}$) as a reference at a scan speed of 0.1 V s^{-1} . Peak potentials are compiled in Table 2 for the cation-radical/neutral porphyrin, neutral porphyrin/radical anion, and radical anion/dianion couples.

The oxidations of tetraphenyl porphyrin **16** and the core-modified porphyrins **4**, **7**, and **8** are quasireversible and irreversible for the others. With the exception of 21-telluraporphyrin **6** and 21-tellura-23-thiaporphyrin **10**, the remaining members of the series have values of E_{ox} within a narrow 0.12 V range (0.98–1.10 V vs Fc/Fc^+). The electrochemical oxidation potential for 21-telluraporphyrin **6** [E_{ox} of +0.81 V (vs Fc/Fc^+), Figure 2a] is more cathodic than E_{ox} for 21-chalcogenaporphyrins **4** and **5** and 21,23-dichalcogenaporphyrins **7–9**, while the oxidation of 21-tellura-23-thiaporphyrin **10** is even more cathodic [E_{ox} of +0.69 V (vs Fc/Fc^+), Figure 2b]. The ease of electrochemical oxidation of **6** and **10** is consistent with the 23-heteroatom facilitating the oxidation of the tellurium atom in the 23-tellurapor-

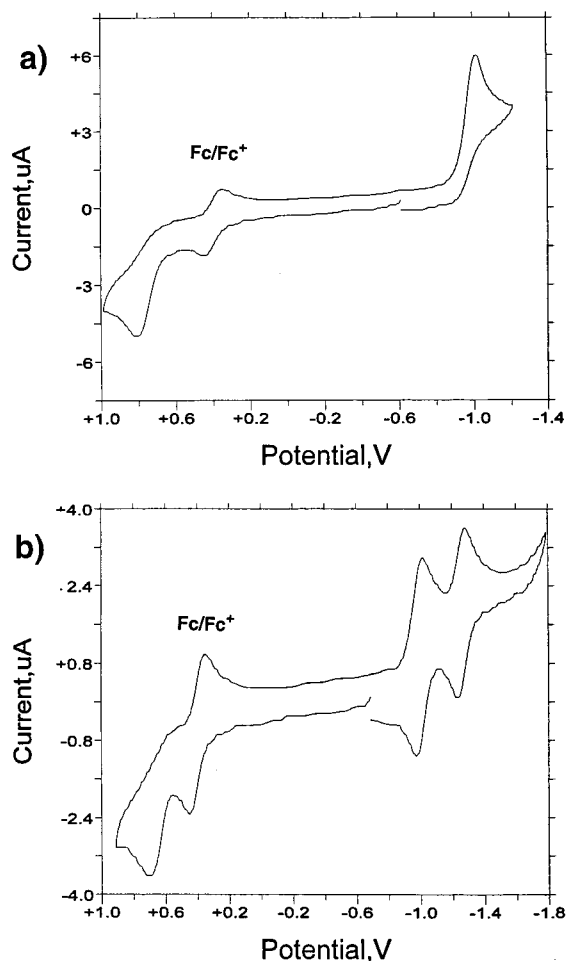


Figure 2. Cyclic voltammograms of (a) 21-telluraporphyrin **6** and (b) 21-tellura-23-thiaporphyrin **10** in dichloromethane with 0.2 M Bu₄NBF₄ as supporting electrolyte at a platinum disk electrode at a scan rate of 0.1 V s⁻¹. Ferrocene was added as internal reference.

phyrins. The oxidation potential of **6** is also consistent with the facile air-oxidation observed for **6** and related compounds.⁴

The first (E_1°) and second (E_2°) reduction potentials for **4**, **5**, **7–10**, and **16** were reversible under our experimental conditions. 21-Telluraporphyrin **6** gave quasireversible reduction waves only at a scan rate of 0.5 V s⁻¹. At a scan rate of 0.1 V s⁻¹, the first reduction wave of **6** was irreversible (Figure 2a). The 21-chalcogen- and 21,23-dichalcogenaporphyrins have first reduction potentials that are more anodic than tetraphenyl porphyrin **16** [E_1° of -1.33 V (vs Fc/Fc⁺) for **16**; E_1° of -1.00 to -1.15 V (vs Fc/Fc⁺) for **4–10**]. The second reduction potentials of 21-chalcogenaporphyrins **4** and **5** and of 21,23-dichalcogenaporphyrins **7–10** are all more anodic than tetraphenyl porphyrin **16** [E_2° of -1.66 V (vs Fc/Fc⁺) for **16**; E_2° of -1.26 to -1.42 V (vs Fc/Fc⁺) for **4**, **5**, and **7–10**]. The second reduction potential of 21-telluraporphyrin **6** [E_2° of -1.61 V (vs Fc/Fc⁺) at 0.5 V s⁻¹] is comparable to that of tetraphenyl porphyrin **16**.

Chemical Oxidation of 21-Telluraporphyrin 6 with Hydrogen Peroxide. Not surprisingly, the same product **12** is formed upon oxidation of **6** with either air or H₂O₂. The addition of H₂O₂ to a solution of **6** in CDCl₃ gave an immediate color change to a dark green

solution, whose ¹H NMR spectrum was identical to that of the product produced by air oxidation of **6**.

The oxidation of **6** was readily monitored spectrophotometrically at 655 nm. At this wavelength, the extinction coefficient increased from 6400 M⁻¹ cm⁻¹ for **6** to 18 100 M⁻¹ cm⁻¹ for **12**. The addition and mixing of 30% H₂O₂ to a cuvette containing 5 × 10⁻⁵ M **6** in ethanol gave a half-life of 5 s with a final H₂O₂ concentration of 5 × 10⁻³ M. Consequently, the second-order rate constant for the oxidation of **6** in ethanol with H₂O₂ is >20 M⁻¹ s⁻¹.

The oxidation of **10** with H₂O₂ was not as clean a reaction as the oxidation of **6**. More than one product was formed, which may be a consequence of oxidation of the sulfur atom as well as the tellurium atom of **10**.

Conclusions

The 21-tellura analogues of 21- and 21,23-core-modified porphyrins have unusual properties relative to their lighter chalcogen analogues. Electrochemical oxidation of **6** and **10** is much more cathodic than oxidation of the lighter chalcogen analogues **4**, **5**, and **7–9**. The more facile oxidation of the organotellurium compounds is reflected in the ease of air-oxidation of 21-telluraporphyrin **6**. We attribute this behavior to the size of the tellurium atom in compounds **6** and **10**, which leads to a distortion from planarity due to 21-tellurium–23-heteroatom interactions in solution. In the crystalline state, a surprisingly planar analogue of **6** has been characterized by X-ray crystallography in which the porphyrin ring is elongated to accommodate the two heteroatoms, which are separated by 3.13 Å.⁴ In contrast, the X-ray crystal structure of **10** has the tellurium atom of the tellurophene ring and the thiophene sulfur at the 23-position tipped in opposite directions, with the tellurophene ring further out of plane than the thiophene ring.^{3b} The 21- and 23-heteroatoms in **10** are separated by only 2.65 Å. As described above, oxidation of **6** gives **12**. An analogue of **12** has also been characterized by X-ray crystallography, and the 21-tellurium atom of the tellurophene ring and the 23-nitrogen atom of the pyrrole ring are also tipped in opposite directions.⁴

The 21-telluraporphyrin analogues have short 21,23-heteroatom contacts. Through-space interaction of a lone-pair of electrons on the 23-heteroatom with the tellurium atom at the 21-position would both facilitate oxidation and stabilize the oxidized product.

The ¹²⁵Te NMR spectra of **6** and **10** are consistent with the effects of shorter intramolecular heteroatom contacts. The Te···S interaction in **10** (2.65 Å Te···S distance)^{3b} is much stronger than the Te···NH interaction in **6** (3.13 Å Te···N distance).⁴ In **10**, the more electronegative sulfur atom would be expected to pull electron density toward it, thus deshielding the more electropositive tellurium atom. The δ 1039 ¹²⁵Te NMR chemical shift for **10** relative to the δ 833 ¹²⁵Te NMR chemical shift for **6** is consistent with increased heteroatom–heteroatom interaction in **10** deshielding the more electropositive tellurium atom.

Oxidation of **6** to **12** gives an expected change in ¹²⁵Te NMR chemical shift for oxidation of Te(II) to Te(IV). The electronegative oxygen and nitrogen atoms and the higher oxidation state deshield tellurium and

increase the ^{125}Te NMR chemical shift from δ 833 in **6** to δ 1045 in **12**.

The oxidation of 21-telluraporphyrin **6** with H_2O_2 proceeds with a second-order rate constant of $>20 \text{ M}^{-1} \text{ s}^{-1}$ presumably due to the participation of the 23-heteroatom. The ease of chemical oxidation is consistent with the properties predicted by the cyclic voltammetry and the spectroscopic properties.

In summary, the 21-telluraporphyrins have excellent properties to make them viable candidates as catalysts for the activation of H_2O_2 . The 23-heteroatom facilitates oxidation and acts as a back door to block approach from one side while forcing oxidizable substrates to approach the tellurium center from one direction only. We are studying the 21-telluraporphyrins **6** and **10**, as well as water-soluble analogues, as catalysts for the activation of H_2O_2 .

Experimental Section

General Methods. Solvents and reagents were used as received from Sigma-Aldrich Chemical Co (St. Louis, MO) unless otherwise noted. Concentration in vacuo was performed on a Büchi rotary evaporator. NMR spectra were recorded at 30.0°C on a Varian Gemini-300, Inova-400, or Inova-500 NMR spectrophotometer with residual solvent signal as internal standard: CDCl_3 (δ 7.26 for proton, δ 77.0 for carbon). Infrared spectra were recorded on a Perkin-Elmer FT-IR instrument. UV-visible-near-IR spectra were recorded on a Perkin-Elmer Lambda 12 spectrophotometer equipped with a circulating constant-temperature bath for the sample chambers. Elemental analyses were conducted by Atlantic Microlabs, Inc. High-resolution Q-TOF mass spectrometry was conducted by the Campus Chemical Instrumentation Center of The Ohio State University (Columbus, OH). Compounds **11a** and **11b** were prepared as described in ref 5a. Compound **11c** was prepared as described in ref 3b.

Preparation of 5,10,15,20-Tetraphenyl-21-thiaporphyrin (4).^{3f} 2,5-Bis(phenylhydroxymethyl)thiophene (**11a**, 1.48 g, 5.00 mmol), benzaldehyde (1.06 g, 10 mmol), and pyrrole (1.00 g, 15 mmol) were dissolved in 1 L of degassed CH_2Cl_2 . Boron trifluoride etherate (0.144 g, 1.0 mmol) and *p*-chloranil (5.68 g, 23 mmol) were added, and the resulting solution was heated at reflux for 1.0 h. The reaction mixture was concentrated to dryness, and the residual solid was purified via chromatography on basic alumina using CH_2Cl_2 as eluent. The first dark red band was collected and the combined fractions were concentrated to give thiaporphyrin **4** as dark purple crystals. Recrystallization from CH_2Cl_2 /hexanes gave 0.38 g (12%) of **4**, mp $>300^\circ\text{C}$; ^1H NMR (CDCl_3) δ 9.74 (s, 2 H), 8.92 (d, 2 H, $J = 3$ Hz), 8.68 (d, 2 H, $J = 3$ Hz), 8.60 (d, 2 H, $J = 3$ Hz), 8.23 (m, 8 H), 7.77 (m, 12 H), -1.6 (1 H); ^{13}C NMR (CDCl_3) δ 157.37, 156.41, 154.40, 147.80, 142.43, 141.21, 138.95, 135.50, 134.55, 134.40, 134.145, 134.06, 131.42, 128.91, 128.03, 127.87, 127.43, 126.62; FT-IR (KBr) 3010, 2977, 1717, 1512, 1370, 1225 cm^{-1} ; FAB(+)-MS, m/z 632 ($\text{C}_{44}\text{H}_{29}\text{N}_3\text{S} + 1$).

Preparation of 5,10,15,20-Tetraphenyl-21-selenaporphyrin (5).^{3f} 2,5-Bis(phenylhydroxymethyl)selenophene (**11b**, 1.72 g, 5.00 mmol), benzaldehyde (1.06 g, 10 mmol), and pyrrole (1.00 g, 15 mmol) were dissolved in 1 L of degassed CH_2Cl_2 . Boron trifluoride etherate (0.144 g, 1.0 mmol) and *p*-chloranil (5.68 g, 23 mmol) were added, and the resulting solution was heated at reflux for 1.0 h. The reaction mixture was concentrated to dryness, and the residual solid was purified via chromatography on basic alumina using CH_2Cl_2 as eluent. The first dark red band was collected and the combined fractions were concentrated to give thiaporphyrin **5** as dark purple crystals. Recrystallization from CH_2Cl_2 /hexanes gave 0.40 g (12%) of **5**, mp $>300^\circ\text{C}$; ^1H NMR (CDCl_3) δ 9.97

(s, 2 H), 8.92 (d, 2 H, $J = 3$ Hz), 8.72 (d, 2 H, $J = 3$ Hz), 8.64 (d, 2 H, $J = 3$ Hz), 8.23 (m, 8 H), 7.77 (m, 12 H), -2.5 (1 H); FT-IR (KBr) 3010, 2977, 1717, 1512, 1370, 1225 cm^{-1} ; FAB(+)-MS, m/z 680 ($\text{C}_{44}\text{H}_{29}\text{N}_3\text{Se} + 1$).

Preparation of 5,10,15,20-Tetraphenyl-21-telluraporphyrin (6). 2,5-Bis(phenylhydroxymethyl)tellurophene (**11c**, 0.98 g, 2.5 mmol), benzaldehyde (0.53 g, 5.0 mmol), and pyrrole (0.50 g, 7.5 mmol) were dissolved in 800 mL of degassed CH_2Cl_2 . Boron trifluoride etherate (0.17 g, 1.2 mmol) was added, and the resulting solution was stirred for 1 h at ambient temperature in the dark. *p*-Chloranil (2.27 g, 9.15 mmol) was then added, and the resulting solution was heated at reflux for 1.0 h in the dark. The reaction mixture was concentrated, and the crude product mixture was purified on basic alumina eluted with dichloromethane. The porphyrin-containing fractions were collected, concentrated, and purified on silica gel eluted with benzene/hexanes. The first dark red band was collected and concentrated. Recrystallization from acetone gave 0.138 g (6.3%) of **6**, mp $>300^\circ\text{C}$; ^1H NMR (CDCl_3) δ 10.44 (s, 2 H), 8.62 (d, 2 H, $J = 1.8$ Hz), 8.60 (d, 2 H, $J = 4.5$ Hz), 8.56 (d, 2 H, $J = 4.5$ Hz), 8.22 (m, 8 H), 7.78 (m, 12 H), -1.60 (br s, 1 H); ^{13}C NMR (CDCl_3) δ 165.03, 160.84, 153.83, 150.42, 142.88, 141.28, 140.44, 136.72, 136.27, 134.78, 134.10, 131.03, 128.10, 127.96, 127.58, 126.66; HR Q-TOF MS, m/z 730.1497 (calcd for $\text{C}_{44}\text{H}_{29}\text{N}_3\text{Te} + \text{H}$, 730.1500). Anal. Calcd for $\text{C}_{44}\text{H}_{29}\text{N}_3\text{Te}$ /acetone (1:1 complex): C, 71.87; H, 4.49; N, 5.35. Found: C, 71.66; H, 4.32; N, 5.44.

Preparation of 5,10,15,20-Tetraphenyl-21,23-dithiaporphyrin (7).^{3a} 2,5-Bis(phenylpyrrolomethyl)thiophene (**15a**) (1.34 g, 3.4 mmol) and 2,5-bis(phenylhydroxymethyl)thiophene (**11a**, 1.01 g, 3.4 mmol) in 1 L of CH_2Cl_2 were treated with tetrachlorobenzoquinone (TCBQ, 4.52 g, 13.6 mmol) and then boron trifluoride etherate (0.17 g, 1.2 mmol) as described above. The crude product was recrystallized from CH_2Cl_2 /MeOH to give 0.375 g (17%) of **7** as a purple solid, mp $>300^\circ\text{C}$; ^1H NMR (CDCl_3 , 300 MHz) δ 9.69 (s, 4 H), 8.69 (s, 4 H), 8.25 (d, 8 H, $J = 7$ Hz), 7.81 (m, 12 H); IR (KBr) 3454, 2915, 2850, 1595, 1458, 1358 cm^{-1} ; FAB(+)-MS, m/z 649 ($\text{C}_{44}\text{H}_{28}\text{N}_2\text{S}_2 + \text{H}$, M + 1). Anal. Calcd for $\text{C}_{44}\text{H}_{28}\text{N}_2\text{S}_2$: C, 81.45; H, 4.35; N, 4.32. Found: C, 81.33; H, 4.32; N, 4.30.

Preparation of 5,10,15,20-Tetraphenyl-21-selena-23-thiaporphyrin (8). 2,5-Bis(phenylpyrrolomethyl)thiophene (**15a**, 1.69 g, 4.30 mmol) and 2,5-bis(phenylhydroxymethyl)selenophene (**11b**, 1.47 g, 4.30 mmol) in 1 L of CH_2Cl_2 were treated with TCBQ (4.41 g, 15.9 mmol) and then boron trifluoride etherate (0.17 g, 1.2 mmol) as described above. The crude product was recrystallized from CH_2Cl_2 /MeOH to give 0.19 g (6%) of **8** as a purple solid, mp $>300^\circ\text{C}$; ^1H NMR (CDCl_3 , 300 MHz) δ 9.94 (s, 2 H), 9.60 (s, 2 H), 8.75 (d, 2 H, $J = 4$ Hz), 8.70 (d, 2 H, $J = 4$ Hz), 8.23 (m, 8 H), 7.80 (m, 12 H); IR (KBr) 3454, 2915, 2850, 1595, 1458, 1358 cm^{-1} ; HR Q-TOF MS, m/z 697.1215 (calcd for $\text{C}_{44}\text{H}_{28}\text{N}_2\text{S}^{80}\text{Se} + \text{H}$, 697.1217). Anal. Calcd for $\text{C}_{44}\text{H}_{28}\text{SSe}$: C, 75.96; H, 4.06; N, 4.03. Found: C, 76.01; H, 4.24; N, 3.99.

Preparation of 5,10,15,20-Tetraphenyl-21,23-diselenaporphyrin (9).^{3a} 2,5-Bis(1-phenyl-1-pyrrolomethyl)selenophene (**15b**) (1.48 g, 3.4 mmol) and 2,5-bis(phenylhydroxymethyl)selenophene (**11b**, 1.17 g, 3.4 mmol) in 1 L of CH_2Cl_2 were treated with TCBQ (4.52 g, 16.4 mmol) and then boron trifluoride etherate (0.17 g, 1.2 mmol) as described above. The crude product was recrystallized from CH_2Cl_2 /MeOH to give 0.303 g (12%) of **9** as a purple solid, mp $>300^\circ\text{C}$; ^1H NMR (CDCl_3 , 300 MHz) δ 9.725 (s, 4 H), 8.72 (s, 4 H), 8.29 (m, 8 H), 7.85 (m, 12 H); IR (KBr) 3454, 2915, 2850, 1595, 1458, 1358 cm^{-1} ; FAB(+)-MS, m/z 745 ($\text{C}_{44}\text{H}_{28}\text{N}_2\text{Se}_2 + 1$).

Preparation of 5,10,15,20-Tetraphenyl-21-tellura-23-thiaporphyrin (10).^{3a} 2,5-Bis(1-phenyl-1-pyrrolomethyl)thiophene (**15a**) (0.90 g, 2.4 mmol) and 2,5-bis(phenylhydroxymethyl)tellurophene (**11b**, 0.96 g, 2.4 mmol) in 800 mL of CH_2Cl_2 were treated with *p*-chloranil (4.52 g, 16.4 mmol) and boron trifluoride etherate (0.17 g, 1.2 mmol) as described

above. The crude product was recrystallized from acetone/MeOH to give 0.034 g (1.9%) of **10** as a purple solid, mp > 300 °C; ¹H NMR (CDCl₃, 300 MHz) δ 10.18 (s, 2 H), 9.08 (s, 2 H), 8.78 (d, 2 H, *J* = 4.8 Hz), 8.71 (d, 2 H, *J* = 4.8 Hz), 8.24 (m, 8 H), 7.74 (m, 12 H); ¹³C NMR (CDCl₃) δ 165.03, 160.39, 157.22, 153.19, 143.14, 142.69, 141.67, 141.43, 140.65, 135.29, 134.64, 134.35, 132.83, 132.53, 128.37, 127.73, 127.43; HR Q-TOF MS, *m/z* 747.1085 (calcd for C₄₄H₂₈N₂S¹³⁰Te + H, 747.1111).

Preparation of 2,5-Bis(1-phenyl-1-pyrrolomethyl)-thiophene (15a). 2,5-Bis(phenylhydroxymethyl)thiophene^{9a} (**11a**, 1.3 g, 4.0 mmol) was dissolved in excess pyrrole (10.6 mL), and argon was bubbled through it. Boron trifluoride etherate was added (0.1 mL), and the resulting mixture was allowed to stir for 1 h. The reaction was stopped by the addition of CH₂Cl₂ (100 mL) followed by 40% NaOH (25 mL). The organic layer was separated, washed with water (3 × 100 mL) and brine (100 mL), dried over MgSO₄, and concentrated. The excess pyrrole was removed via vacuum distillation at ambient temperature. The residual oil was purified via chromatography on silica gel eluted with 75:25 hexanes/ethyl acetate. The yellow band was collected to give a yellow oil, which was recrystallized from ethyl acetate/hexanes to give 0.74 g (46%) of **15a** as a white solid, mp 98–100 °C; ¹H NMR (CDCl₃, 300 MHz) δ 7.91 (br s, 2 H, N–H), 7.34 (t, 4 H, *J* = 5 Hz), 7.28 (d, 6 H, *J* = 3 Hz), 6.71 (s, 2 H), 6.60 (s, 2 H), 6.17 (q, 2 H, *J* = 2 Hz), 5.95 (s, 2 H), 5.59 (s, 2 H); ¹³C NMR (CDCl₃, 75 MHz) δ 145.82, 142.61, 132.98, 128.57, 128.55, 127.05, 125.34, 117.22, 108.29, 107.51, 45.96; IR (KBr) 3510, 2978, 1716, 1521, 1363, 1222 cm⁻¹; FAB(+)/MS, *m/z* 395 (C₂₆H₂₂N₂S + H, M⁺ + 1). Anal. Calcd for C₂₆H₂₂N₂S: C, 79.15; H, 5.62; N, 7.11. Found: C, 79.06; H, 5.64; N, 6.87.

Preparation of 2,5-Bis(1-phenyl-1-pyrrolomethyl)-selenophene (15b). 2,5-Bis(phenylhydroxymethyl)-selenophene^{9b} (**11b**, 1.21 g, 3.5 mmol) and pyrrole (10.8 mL) were treated with boron trifluoride etherate (0.1 mL) as described. The residual oil was purified via chromatography on silica gel eluted with 75:25 hexanes/ethyl acetate and was recrystallized from ethyl acetate/hexanes to give 0.70 g (51%) of **15b** as a white solid, mp 109–111 °C; ¹H NMR (CDCl₃) δ 8.08 (br s, 2 H, N–H), 7.45 (m, 10 H, Ar), 6.97 (s, 2 H), 6.86 (s, 2 H), 6.32 (q, 2 H, *J* = 2 Hz), 6.14 (s, 2 H), 5.77 (s, 2 H); ¹³C NMR (CDCl₃, 75 MHz) δ 153.51, 143.01, 133.34, 128.61, 128.34, 127.46, 127.07, 117.17, 108.31, 107.44, 48.10; IR (KBr) 3426, 1700, 1628, 1457 cm⁻¹; FAB(+)/MS, *m/z* 443 (C₂₆H₂₂N₂-80Se + H, M + 1). Anal. Calcd for C₂₆H₂₂N₂Se: C, 70.79; H, 5.02; N, 6.35. Found: C, 70.91; H, 5.13; N, 6.25.

Electrochemical Procedures. A BAS 100 potentiostat/galvanostat and programmer were used for the electrochemical measurements. The working electrode for cyclic voltammetry was a platinum disk electrode (diameter, 1 mm) obtained from Princeton Applied Research. The auxiliary and reference electrodes were silver wires. The reference for cyclic voltam-

metry was the Fc/Fc⁺ couple at +0.40 V at a scan rate of 0.1 V s⁻¹. All samples were run in HPLC-grade dichloromethane (Aldrich Chemical Co.) that had been stored over 3 Å molecular sieves and freshly distilled prior to use. Tetrabutylammonium fluoroborate (Aldrich Chemical Co.) was recrystallized from ethyl acetate/ether and then dried overnight at 80 °C before it was used as supporting electrolyte at 0.2 M. Nitrogen was used for sample deaeration.

Oxidation of 6 To Give 21-Oxo-21-telluraporphyrin 12. A solution of 3.0 mg of **6** in 1.5 mL of CDCl₃ in a 5 mm NMR tube was allowed to stand in air. The progress of oxidation was followed by ¹H NMR. After 24 h, the reaction was complete. The ¹H NMR spectrum was collected, and then the sample was concentrated to give a purple solid, mp > 300 °C; ¹H NMR (CDCl₃) δ 10.50 (s, 2 H), 8.47 (d, 2 H, *J* = 4.4 Hz), 8.44 (d, 2 H, *J* = 4.4 Hz), 8.31 (br s, 2 H), 8.25 (m, 4 H), 8.12 (m, 2 H), 8.11 (m, 2 H), 7.9–7.6 (m, 12 H); ¹²⁵Te NMR (CDCl₃) δ 1045; HR Q-TOF MS, *m/z* 746.1446 (calcd for C₄₄H₂₉N₃O¹³⁰Te + H, 746.1451).

For the acquisition of the ¹²⁵Te NMR spectrum, the air-oxidation of a solution of 20 mg of **6** in 1.0 mL of CDCl₃ was slow (<10% reaction to **12** after 48 h). The addition of 20 μL of 30% H₂O₂ immediately gave a dark green solution, whose ¹H NMR spectrum was identical to that of the air-oxidation product. This sample was used to collect the ¹²⁵Te NMR data.

Acquisition of ¹²⁵Te NMR Spectra. The NMR samples were prepared in CDCl₃ in 5 mm NMR tubes. The ¹²⁵Te NMR spectra were recorded on a Varian Inova-400 NMR spectrometer at 126.289 MHz and 55 °C. The spectral width for acquisition was set to 320 kHz with an acquisition time of 0.82 s. The data were collected for 16K transients, with a pulse width of 9 μs and a relaxation delay of 3–4 s. The FIDs were transformed with an exponential line broadening function of 10–15 Hz. Samples were referenced relative to 2,6-diphenyl-telluropyran-4-one as an external standard with a chemical shift of δ 553 relative to Me₂Te (δ 0.0).¹¹

Acknowledgment. The authors thank the National Science Foundation and the Petroleum Research Fund, administered by the American Chemical Society, for grants in support of this work. The authors also thank Prof. Jerome B. Keister for his assistance in acquiring the electrochemical data.

Supporting Information Available: Electronic absorption spectra for compounds **6**, **7**, **9**, **10**, and **12**. This information is available free of charge via the Internet at <http://pubs.acs.org>.

OM0202219

(11) Detty, M. R.; Lenhart, W. C.; Gassman, P. G.; Callstrom, M. R. *Organometallics* **1989**, *8*, 861.